

# On the formation of Hubble flow in Little Bangs

Mikołaj Chojnacki\*

*Institute of Physics, Świętokrzyska Academy, PL-25406 Kielce, Poland*

Wojciech Florkowski†

*Institute of Physics, Świętokrzyska Academy, PL-25406 Kielce, Poland and  
Institute of Nuclear Physics, Polish Academy of Sciences, PL-31342 Kraków, Poland*

Tamás Csörgő‡

*MTA KFKI RMKI, H-1525 Budapest 114, P. O. Box 49, Hungary*

(Dated: October 7, 2004)

A dynamical appearance of scaling solutions in the relativistic hydrodynamics applied to describe ultra-relativistic heavy-ion collisions is studied. We consider the boost-invariant cylindrically symmetric systems and the effects of the phase transition are taken into account by using a temperature dependent sound velocity inferred from the lattice simulations of QCD. We find that the transverse flow acquires the scaling form  $r/t$  within the short evolution times, 10-15 fm, only if the initial transverse flow originating from the pre-equilibrium collective behavior is present at the initial stage of the hydrodynamic evolution. The amount of such pre-equilibrium flow is correlated with the initial pressure gradient; larger initial gradients require smaller initial flow. The results of the numerical calculations support the phenomenological parameterizations used in the Blast-Wave, Buda-Lund, and Cracow models of the freeze-out process.

PACS numbers: 25.75.Dw, 21.65.+f, 14.40.-n

## I. INTRODUCTION

Hadronic data collected in the heavy-ion experiments at RHIC support the idea that the system formed in Au+Au collisions is highly thermalized and undergoes strong transverse and longitudinal expansion [1]. Moreover, successful parameterizations of the freeze-out process indicate that such expansion may be characterized by the Hubble law [2, 3, 4]. In the simplest form, used in cosmology, this law states the proportionality of the relative velocity of galaxies to their relative separation,

$$\mathbf{v} = H\mathbf{r}. \quad (1)$$

The constant of proportionality or Hubble's constant  $H$  is a function of time. In the Friedmann universe [5] as well as in analytic solutions of non-relativistic fireball hydrodynamics [6], its value is

$$H = \frac{\dot{R}}{R}, \quad (2)$$

where the function  $R(t)$  is in general a complicated function of time. In nuclear hydrodynamics, the Hubble law characterizes the fluid velocity distributions of the expanding matter, while in cosmology the Hubble law characterizes the expansion of the space. In the non-relativistic hydrodynamics, the scale parameter  $R(t)$  depends on the initial conditions as well as on the equation of state, while in cosmology the time evolution of the scale parameter  $R$  depends not only on the initial conditions (flat, open or closed universe) and the properties of matter (matter dominated and radiation dominated epoch) but also on the possible existence of dark energy and cosmological constants, and the possible presence of an exponentially accelerating, inflationary period. At the end of the accelerating period, when  $\dot{R} = \text{const.}$  and  $R \approx \dot{R}t$ , the Hubble constant is simply the inverse of the lifetime,  $H = 1/t$ .

At the very end of fireball explosions, the pressure decreases to vanishing values, hence the acceleration caused by pressure gradients becomes negligibly small. In this case, the Hubble law connects the hydrodynamic flow four-velocity

---

\*Electronic address: chojnacki@mikolaj@tlen.pl

†Electronic address: florkows@amun.ifj.edu.pl

‡Electronic address: csorgo@sunserv.kfki.hu

$u^\mu$  with the space-time position of the fluid element  $x^\mu$ , in a simple way,

$$u^\mu = \frac{x^\mu}{\tau} = \frac{t}{\tau} \left( 1, \frac{x}{t}, \frac{y}{t}, \frac{z}{t} \right). \quad (3)$$

The quantity  $\tau$  in Eq. (3) is the proper time characterizing the freeze-out hypersurface,

$$\tau = \sqrt{t^2 - r^2 - z^2}, \quad r = \sqrt{x^2 + y^2}. \quad (4)$$

Clearly, the parameterization (3) - (4) makes sense in the space-time region defined by the condition  $r^2 + z^2 < t^2$ . The three-velocity field of the form

$$\mathbf{v} = \left( \frac{x}{t}, \frac{y}{t}, \frac{z}{t} \right), \quad (5)$$

following directly from Eq. (3), appears very often in the analysis of the hydrodynamic equations applied to describe hadronic or nuclear collisions. In this context it is called the asymptotic *scaling solution* [7, 8, 9, 10, 11, 12]. In particular, for the boost-invariant systems the longitudinal velocity must be of the form  $v_z = z/t$ , which is a direct consequence of the Lorentz symmetry [11, 13, 14, 15, 16, 17]. It is often believed, that during the pre-equilibrium period of high energy nuclear collisions, no significant transverse flow is generated (for recent reviews of the hydrodynamic description of relativistic heavy-ion collisions see, e.g., Refs. [18, 19, 20, 21]). In such a case, the transverse fluid velocity builds up during the hydrodynamic evolution of the system [12] and the scaling form  $v_r = r/t$  may be reached only for sufficiently large times (with details depending on the equation of state and initial conditions). Similar features characterize also a spherically symmetric expansion of the system being initially at rest. In this case, the radial flow is formed by the outward action of the pressure gradient, and the numerical calculations show that Eq. (3) is the asymptotic solution [10, 12].

In view of the success of the fits [2, 4, 28, 29] which all indicate very strong transverse flows, one of the central issues is whether the times actually available in relativistic heavy-ion collisions are sufficient to allow for a dynamical development of such strong transverse flows, in particular, the scaling solutions corresponding to Eq. (3). The situation is especially intriguing for RHIC, where several measurements indicate an unexpected, rather short (about 10 - 15 fm) duration time of the collision process. For example, one finds  $\tau \sim 10$  fm using the RHIC data in the relation  $R_L(m_T) = \tau \sqrt{T_k/m_T}$  [30], which connects the longitudinal pion correlation radius  $R_L$ , the kinetic freeze-out temperature  $T_k$ , the evolution time  $\tau$ , and the transverse mass of the pion pair  $m_T$ .

These measurements, when interpreted with care, yield only the inverse of the (longitudinal) Hubble constant, which can be identified with the lifetime only if the scaling solution is assumed to be developed in the longitudinal direction. This situation is analogous to the estimate of the lifetime of the Universe: the inverse of the presently measured value of the Hubble constant yields an order-of-magnitude estimate of the lifetime, which has to be corrected for the effects of inflation and possible other acceleration periods. Similarly, in nuclear hydrodynamics, there is an initial longitudinal acceleration period, hence the estimated lifetimes should be interpreted only as (lower) limits on the total lifetime of the system [4].

Many hydrodynamic codes used to describe the heavy-ion data show that the scaling solutions do not appear before the freeze-out of the system. However, such approaches assume commonly that the initial transverse flow is zero. An exception from this rule is the work by Kolb and Rapp [31], where the pre-equilibrium transverse flow is considered and its presence improves the agreement of the model calculations with the data. Another important exception is a class of the non-relativistic, selfsimilar solutions of the fireball hydrodynamics, which is by now solved completely in the ellipsoidally symmetric case for arbitrary initial sizes and expansion velocities of the principal axes of the expanding ellipsoids [32], arbitrary initial temperature profiles [33], as well as for arbitrary (temperature dependent) speed of sound [34].

In this paper we follow such ideas and assume that the elementary parton-parton collisions, leading to the thermalization of the system, lead also to collective behavior and development of the transverse flow already at the initial stage of the equilibrium hydrodynamic evolution at the time  $t = t_0 \sim 1$  fm. For simplicity, we consider the boost-invariant and cylindrically symmetric systems with the initial transverse flow defined by the formula

$$v_r^0 = v_r(t = t_0, r) = \frac{Hr}{\sqrt{1 + H^2 r^2}}. \quad (6)$$

The parameter  $H$  in Eq. (6) may be interpreted as the Hubble constant which determines the magnitude of the initial transverse flow; in the range  $r < 1/H$  the flow is well approximated by the linear function  $v_r^0 \sim Hr$ , whereas for  $r > 1/H$  the flow approaches the speed of light, a boundary condition frequently assumed in the hydrodynamic equations for large values of  $r$  [12]. Also, if the above equation is specified on a hypersurface corresponding to a constant proper-time, it coincides with the Hubble law of Eq. (3).

By varying the value of  $H$  we control the amount of the initial transverse flow which may possibly develop into the scaling form (5). We note that in the scaling solution (5) the role of the Hubble constant is played by the inverse of the time coordinate  $t$ . This means that setting  $H = 1/t_0 = 1\text{fm}^{-1}$  we assume that the initial flow is already very close to the scaling form at  $t_0$ . In this particular case the question arises if the flow remains close to the scaling form in the subsequent time evolution of the system.

A few comments are in order now. Following the conventional hydrodynamic approach [12], we specify the initial conditions at a constant time,  $t_0 = 1\text{ fm}$ , and search for the solutions which are regular functions of  $t$  and  $r$  in the region:  $t > t_0$ ,  $r > 0$ . In this case, at a given value of time  $t$ , the scaling solution cannot hold for arbitrary large values of  $r$ , since this would yield the flow velocities larger than the speed of light, and also the initial condition deviates from Eq. (1) for large values of the transverse radius. Hence, in our analysis we search for the solutions of the hydrodynamic equations which yield the flow profiles possibly close to the scaling solution in the region  $r < t$ . In a separate paper we intend to explore a different type of the initial conditions, which are specified at a fixed value of the proper time and lead, in certain special cases, to the exact solutions given in Refs. [26, 27]. We also note that in view of the recent BRAHMS data [35, 36] describing rapidity dependence of hadron production, the boost-invariant approach assumed in the present calculation may be appropriate only if limited to the rapidity range:  $-1 < y < 1$ .

## II. CHARACTERISTIC FORM OF THE HYDRODYNAMIC EQUATIONS

In this Section we introduce the basic notation and rewrite the hydrodynamic equations in the form convenient for the numerical calculations. We follow closely the method introduced by Baym, Friman, Blaizot, Soyeur, and Czyż [12]. We restrict our considerations to the systems with zero net baryon density, which is a good approximation for description of the central rapidity region at the RHIC energies (thermal analysis of the ratios of hadron multiplicities indicates that the baryon chemical potential at RHIC energies is about 30 MeV, i.e., it is much smaller than the corresponding temperature of about 170 MeV [4, 37, 38]). In this case the hydrodynamic equations have the form

$$u^\mu \partial_\mu (T u^\nu) = \partial^\nu T, \quad (7)$$

$$\partial_\mu (\sigma u^\mu) = 0, \quad (8)$$

where  $T$  is the temperature,  $\sigma$  is the entropy density, and  $u^\mu = \gamma(1, \mathbf{v})$  is the hydrodynamic four-velocity (with  $\gamma = 1/\sqrt{1 - v^2}$ ). Eq. (7) is the acceleration equation which is the analog of the Euler equation of the classical hydrodynamics, whereas Eq. (8) represents entropy conservation (the adiabaticity of the flow). Since  $T$  is the only independent thermodynamic variable, all other thermodynamic quantities can be obtained from the equation of state  $P(T)$ , connecting pressure  $P$  with the temperature  $T$ . With the help of the thermodynamic relations

$$d\varepsilon = T d\sigma, \quad dP = \sigma dT, \quad w = \varepsilon + P = T\sigma, \quad (9)$$

other thermodynamic quantities, such as the energy density  $\varepsilon$  or the enthalpy density  $w$ , can be obtained. In addition, the equation of state allows us to calculate the sound velocity

$$c_s^2 = \frac{\partial P}{\partial \varepsilon} = \frac{\sigma}{T} \frac{\partial T}{\partial \sigma}. \quad (10)$$

Equation (8) and the spatial components of Eq. (7) may be rewritten for the boost invariant systems with cylindrical symmetry as

$$v_r \frac{\partial \ln T}{\partial t} + \frac{\partial \ln T}{\partial r} + \frac{\partial \alpha}{\partial t} + v_r \frac{\partial \alpha}{\partial r} = 0, \quad (11)$$

$$\frac{\partial \ln \sigma}{\partial t} + v_r \frac{\partial \ln \sigma}{\partial r} + v_r \frac{\partial \alpha}{\partial t} + \frac{\partial \alpha}{\partial r} + \frac{1}{t} + \frac{v_r}{r} = 0, \quad (12)$$

where  $\alpha$  is the transverse rapidity of the fluid defined by the condition  $v_r = \tanh \alpha$ . The longitudinal component has the well known boost-invariant form  $v_z = z/t$  [11].

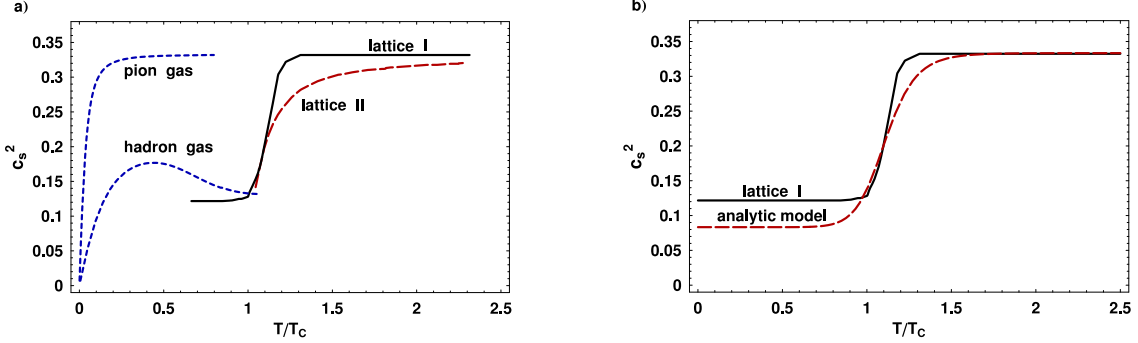


FIG. 1: **a)** Temperature dependence of the sound velocity as obtained from different theoretical models described in the text. **b)** Sound velocity used in this calculation: the solid line describes the lattice result, i.e., the function "lattice I" from part a) extrapolated to low temperatures, whereas the dashed line describes the analytic model defined by Eq. (21).

By introducing the potential  $\Phi(T)$  defined by the differentials

$$d\Phi = \frac{d \ln T}{c_s} = c_s d \ln \sigma, \quad (13)$$

and by the use of the two functions  $a_{\pm}$  defined by the formula

$$a_{\pm} = \exp(\Phi \pm \alpha), \quad (14)$$

Eqs. (11) and (12) may be cast into the characteristic form [12]

$$\frac{\partial}{\partial t} a_{\pm}(t, r) + \frac{v_r \pm c_s}{1 \pm v_r c_s} \frac{\partial}{\partial r} a_{\pm}(t, r) + \frac{c_s}{1 \pm v_r c_s} \left( \frac{v_r}{r} + \frac{1}{t} \right) a_{\pm}(t, r) = 0. \quad (15)$$

If the functions  $a_{\pm}$  are known, the potential  $\Phi$  may be calculated from the formula

$$\Phi = \frac{1}{2} \ln (a_+ a_-), \quad (16)$$

and the velocity is obtained from the equation

$$v_r = \frac{a_+ - a_-}{a_+ + a_-}. \quad (17)$$

The knowledge of the function  $c_s(T)$  allows us, by the integration of Eq. (13), to determine  $\Phi$  as a function of the temperature; this function will be called later  $\Phi_T$ . However, to get a closed system of equations for  $a_+$  and  $a_-$ , we have to invert this relation and obtain  $T$  as a function of  $\Phi$ ; this function will be called later  $T_{\Phi}$ . In this way, the sound velocity may be expressed in terms of the functions  $a_+$  and  $a_-$ ,

$$c_s = c_s \left[ T_{\Phi} \left( \frac{1}{2} \ln (a_+ a_-) \right) \right], \quad (18)$$

and Eqs. (15) may be solved numerically.

### III. TEMPERATURE DEPENDENT SOUND VELOCITY

In our numerical calculations we take into account the temperature dependence of the sound velocity. In this way, we generalize the approach of Ref. [12], where Eqs. (15) - (17) were solved numerically only in the case  $c_s^2 = 1/3$ . The results of different model calculations of the sound velocity, which may serve as the input for the hydrodynamic calculations are presented in Fig. 1 a). The solid line (denoted as "lattice I") is the result of Mahony and Alam [39],

who compiled the lattice results obtained by Karsch [40] in order to get  $c_s(T)$  from the temperature dependence of the energy density. The long-dashed line (denoted as "lattice II") shows the result of the lattice QCD calculations by Szabó and Tóth [41].

A sudden but smooth change of the sound velocity in the small temperature range around  $T = T_c$ , as observed in the lattice calculations, see Fig. 1 a), indicates a rapid cross-over from a hadron gas to a quark-gluon plasma phase. Above the critical temperature, ( $T \gg T_c$ ) the sound velocity approaches the limit valid for massless particles,  $c_s^2 = 1/3$ , whereas below the phase transition ( $T \ll T_c$ ) the sound velocity is much smaller, being close to the value obtained for the case of the noninteracting gas of hadron resonances.

The hadron-gas result shown in Fig. 1 a) was obtained by us in the calculation which uses the recent fits to the meson and baryon mass spectra [42, 43, 44] denoted below by  $\rho_M(m)$  and  $\rho_B(m)$ . One possible parameterization of the spectra [43], which reveals directly their exponential growth, as suggested long ago by Hagedorn [45], is as follows

$$\begin{aligned}\rho_M(m) &= a_M \exp(m/T_M), \quad a_M = 4.41 \text{ GeV}^{-1}, \quad T_M = 311 \text{ MeV}, \\ \rho_B(m) &= a_B \exp(m/T_B), \quad a_B = 0.11 \text{ GeV}^{-1}, \quad T_B = 186 \text{ MeV}.\end{aligned}\quad (19)$$

With the help of the mass distributions (19), we calculate the entropy density of the hadron gas as a sum over contributions from all known hadronic states from the formula

$$\sigma(T) = \frac{1}{2\pi^2} \int_{m_{\text{pion}}}^{M_{\text{mesons}}^{\text{max}}} \rho_M(m) m^3 K_3\left(\frac{m}{T}\right) dm + \frac{2}{2\pi^2} \int_{m_{\text{nucleon}}}^{M_{\text{baryons}}^{\text{max}}} \rho_B(m) m^3 K_3\left(\frac{m}{T}\right) dm. \quad (20)$$

The sound velocity of the hadron gas follows then directly from the use of Eq. (20) in (10). Eq. (20) is valid in the case of zero baryon chemical potential and the factor 2 in the second term accounts for antibaryons. The effects of the quantum statistics (Bose-Einstein or Fermi-Dirac) are neglected in Eqs. (20), because they are known to be small; of the order of 20% or less for reasonable range of the temperatures [8]. To match our hadron-gas calculation with the lattice data we assumed that the critical temperature is 170 MeV. The upper limits of the integrations in (20) are  $M_{\text{mesons}}^{\text{max}} = 2.3$  GeV for mesons and  $M_{\text{baryons}}^{\text{max}} = 1.8$  GeV for baryons. These limits are determined by the range where the fit (19) works well [44]; for higher masses, due to the lack of data, the spectra saturate.

For comparison, in Fig. 1 a) we show the speed of sound obtained in the similar calculation where the massive pions are included only. The speed of sound in the pion gas reaches very fast the limiting value of  $1/\sqrt{3}$ , which may be confronted with the non-monotonic behavior of  $c_s$  in the gas of resonances. Similar behavior of the speed of sound in the gas of resonances was found also in the case with non-zero baryon density [46]. It is interesting to note that the lattice data agree with the hadron-gas calculation close to the phase transition region if we assume  $T_c \sim 170$  MeV. Moreover, the speed of sound in the hadron resonance gas below the critical temperature is found to be significantly smaller than  $1/\sqrt{3}$ , which is the limit of massless ideal relativistic gas used in the bag model type of the equations of state. As the hydrodynamic equations describe the properties of matter through the equation of state, or more precisely through the speed of sound [8], such decrease of the speed of sound in the hadron gas stage, compared to the massless pion gas limit, changes drastically the corresponding time evolution of the hydrodynamic solutions.

Although the calculations of the speed of sound shown in Fig. 1 a) are based on the observed hadron mass spectra below  $T_c$  and on the lattice QCD above  $T_c$ , they are still somewhat ambiguous and not completely satisfactory. For example, lattice QCD calculations below the critical temperature still yield too heavy pions, and we know that the value of the speed of sound is rather sensitive to the pion mass. On the other hand, the calculation based on the Hagedorn mass spectrum in the hadronic phase is more realistic than the lattice results in the low temperature domain, however, it neglects the role of interactions between the hadrons.

In this situation, we decided to use as the main input the equation of state (sound velocity) delivered by Ref. [39], which is shown as "lattice I" in Fig. 1 a). This calculation is based on first principles and extends down to about  $0.6 T_c$ , i.e., to the low-temperature region of about 100 MeV relevant for the discussions of the kinetic freeze-out. In the actual calculation we extrapolate this result to even lower temperatures as shown in Fig. 1 b). We also use an analytic form of the function  $c_s(T)$  which exhibits the main features observed in Fig. 1 a) and, at the same time, leads to the analytic expressions for the functions  $\Phi_T(T)$  and  $T_\Phi(\Phi)$ . This function is defined by the formula

$$c_s(T) = \frac{1}{\sqrt{3}} \left[ 1 - \frac{1}{2} \left( \frac{1}{1 + (T/\tilde{T})^{2n}} \right) \right]. \quad (21)$$

Using Eq. (21) one finds  $c_s(T) = 1/\sqrt{3}$  for  $T \gg \tilde{T}$  and  $c_s(T) = 1/(2\sqrt{3})$  for  $T \ll \tilde{T}$ . A straightforward integration of Eq. (13) gives in this case

$$\Phi_T(T) = \frac{\sqrt{3}}{2n} \ln \frac{(T/\tilde{T})^{4n}}{1 + 2(T/\tilde{T})^{2n}} \quad (22)$$

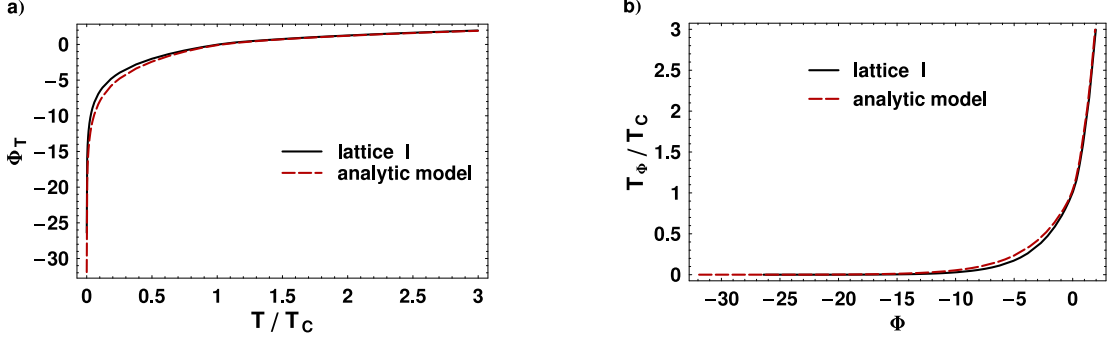


FIG. 2: **a)** The potential  $\Phi$  obtained by the integration of Eq. (13). **b)** Temperature as a function of the potential  $\Phi$ . In both cases, a) and b), the solid lines show the results obtained with the lattice equation of state, whereas the dashed lines describe the analytic model defined by Eq. (21).

and

$$T_\Phi(\Phi) = \tilde{T} \left[ e^{\frac{2n\Phi}{\sqrt{3}}} + \sqrt{e^{\frac{2n\Phi}{\sqrt{3}}} + e^{\frac{4n\Phi}{\sqrt{3}}}} \right]^{\frac{1}{2n}}. \quad (23)$$

With the parameters  $\tilde{T} = 1.08 T_c$  and  $n = 6$  the function (21) well approximates the lattice results I and II in the region slightly above  $T_c$ , and interpolates between the lattice results I and II at higher temperatures. At low temperatures,  $T < 0.6 T_c$ , the function (21) behaves like a constant, see Fig. 1 b). The functions  $\Phi_T(T)$  and  $T_\Phi(\Phi)$ , defined by Eqs. (22) and (23) with  $\tilde{T} = 1.08 T_c$  and  $n = 6$  are represented in Fig. 2 by the dashed lines. The solid lines in Fig. 2 show the same functions obtained for the lattice case. (*In the following, we shall refer to the lattice calculations having in mind the case "lattice I", including a linear extrapolation at very low temperatures*).

#### IV. INITIAL CONDITIONS

From the symmetry reasons, the velocity field should vanish at  $r = 0$ . This condition is achieved if the functions  $a_+$  and  $a_-$  are initially determined by a single function  $a(r)$  according to the prescription [12]

$$a_+(t = t_0, r) = a(r), \quad a_-(t = t_0, r) = a(-r). \quad (24)$$

In the following we shall assume that the hydrodynamic evolution starts at a typical time  $t = t_0 = 1$  fm. We shall also assume that the initial temperature profile is connected with the nucleon-nucleus thickness function  $T_A(r)$ ,

$$T(t = t_0, r) = \text{const } T_A^{1/3}(r). \quad (25)$$

where

$$T_A(r) = 2 \int d^2s \int dz \rho \left( \sqrt{(\mathbf{s} - \mathbf{r})^2 + z^2} \right). \quad (26)$$

Here the function  $\rho(r)$  is the nuclear density profile given by the Woods-Saxon function with a conventional choice of the parameters ( $\rho_0 = 0.17 \text{ fm}^{-3}$ ,  $r_0 = (1.12A^{1/3} - 0.86A^{-1/3}) \text{ fm}$ ,  $a = 0.54 \text{ fm}$ ,  $A = 197$ ).

The idea to use Eq. (25) follows from the assumption that the initially produced entropy density  $\sigma(r)$  is proportional to the number of the nucleons participating in the collision at a distance  $r$  from the collision center [19],  $\sigma(r) \sim T_A(r)$ . Since for massless particles the entropy density is proportional to the third power of the temperature, we arrive at Eq. (25).

We note that other choices for the initial temperature profile are also conceivable. If we assume that the initially produced energy density is proportional to the nuclear thickness function, instead of Eq. (25) we obtain

$$T(t = t_0, r) = \text{const } T_A^{1/4}(r). \quad (27)$$

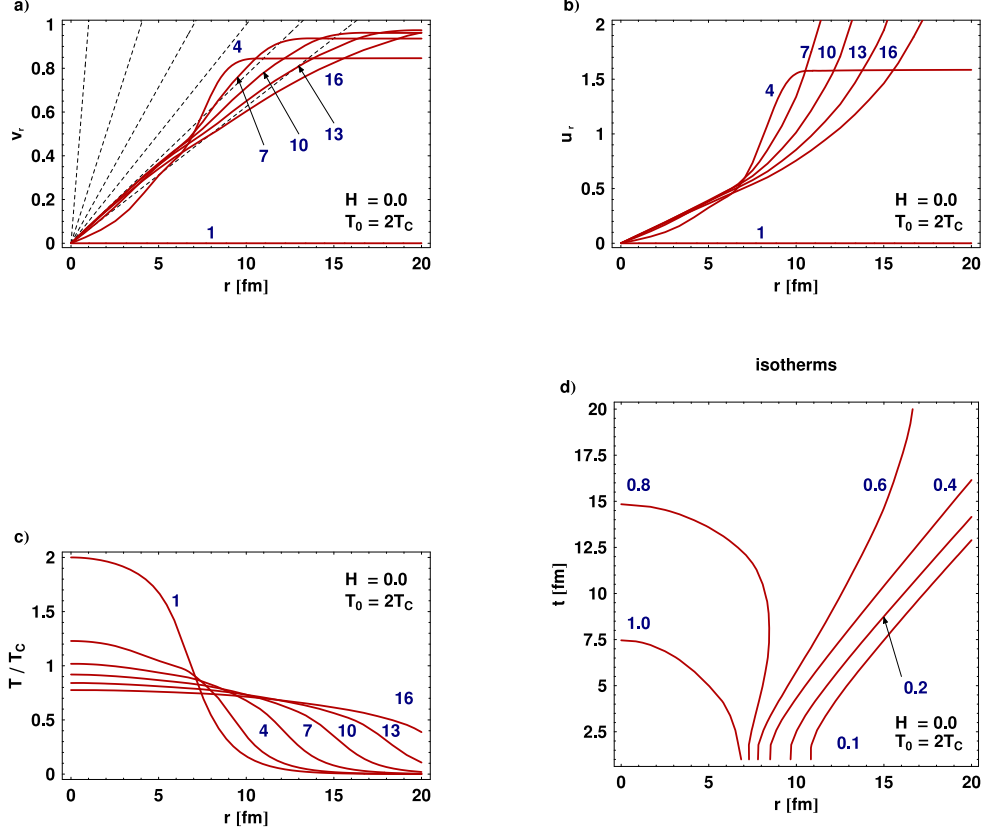


FIG. 3: Hydrodynamic expansion of matter being initially at rest, i.e., in the case  $H = 0$ . The initial central temperature  $T_0 = 2T_c$ . The part **a**) shows the transverse velocity as a function of the distance from the center for 6 different values of time,  $t_i = 1, 4, 7, 10, 13$  and  $16$  fm. The dashed thin lines describe the ideal Hubble-like profiles of the form  $r/t_i$  ( $r < t_i$ ). The part **b**) shows the transverse four-velocity as a function of  $r$  for the same values of time. The part **c**) shows the temperature profiles in  $r$  whereas the part **d**) shows the isotherms in the  $t - r$  space. In this case, the labels at the curves denote the values of the temperature in units of the critical temperature.

If we assume that the energy deposition into the thermalization is driven by the collisions of wounded nucleons, and every collision contributes with certain probability distribution to a local increase of the temperature, then after many collisions the central limit theorem may describe the form of the local temperature distribution and this is a Gaussian form. However, if there are big fluctuations in the deposited energy, the generalized central limit theorems apply and in this case the local temperature distribution may have the generalized, Lévy stable form. As a special case, the Lorentzian temperature profile can also be obtained.

The two initial conditions (6) and (25) may be included in the initial form of the function  $a(r)$  if we define

$$a(t = t_0, r) = a_T(r) \frac{\sqrt{1 + v_r^0}}{\sqrt{1 - v_r^0}}, \quad (28)$$

where

$$a_T(r) = \exp \left[ \Phi_T \left( \text{const } T_A^{\frac{1}{3}}(|r|) \right) \right]. \quad (29)$$

## V. RESULTS

It is important to observe, that the Hubble law  $v = Hr$  is satisfied in the  $r \ll t$  region after  $t = 7$  fm in all the cases that we explored numerically in the present calculation, regardless of the initial conditions. However, the value

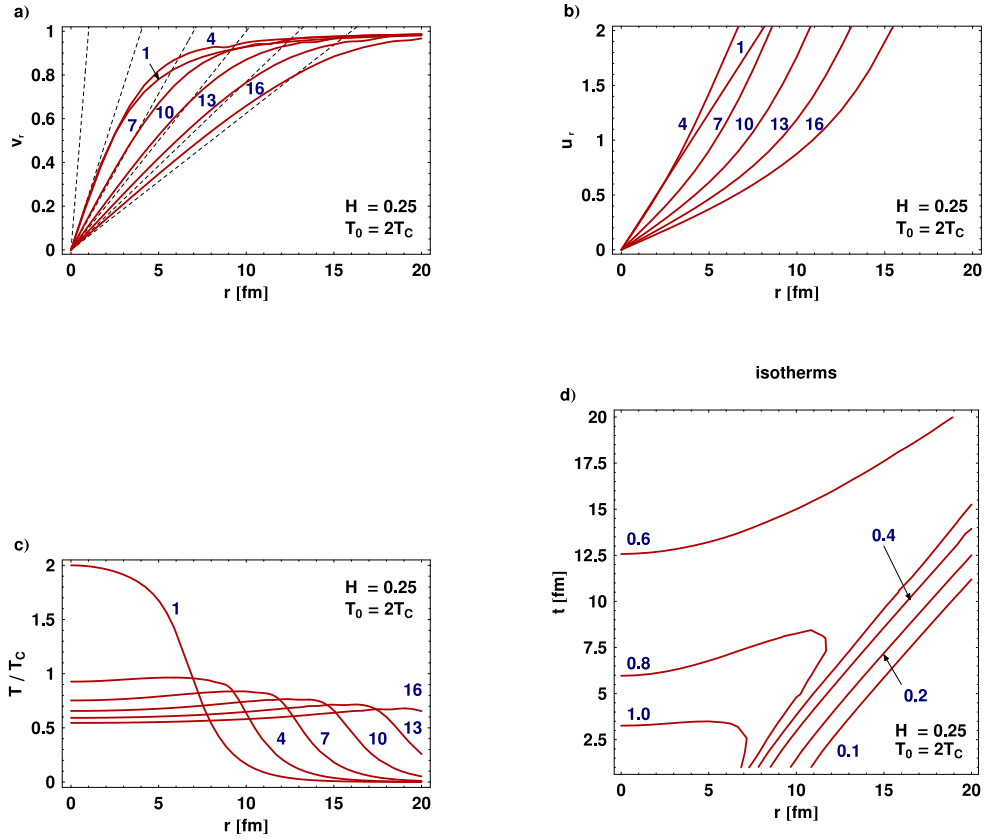


FIG. 4: Hydrodynamic expansion of matter with initial pre-equilibrium flow characterized by the velocity profile (6) with  $H = 0.25$ . The initial central temperature  $T_0 = 2T_c$ . Notation as in Fig. 3.

of the Hubble constant typically deviates from the inverse of time, which signals that the asymptotic form of the Hubble flow, eq. (3) is reached only after a longer time period. The onset of the asymptotic scaling is determined by the initial conditions as we shall detail below.

In Figs. 3 and 4 we show our results obtained for two different initial conditions characterized by the two different values of the parameter  $H$ ,  $H = 0$  and  $H = 0.25 \text{ fm}^{-1}$ , respectively. In both cases the lattice equation of state is used and the initial temperature in the center of the system is assumed to be twice the temperature of the phase transition,  $T_0 = T(t = t_0, r = 0) = 2T_c$ . This means, that for the commonly accepted value of  $T_c$ , which is about 170 MeV, the initial temperature in the center reaches about 340 MeV.

In the case  $H = 0$ , the transverse flow is initially set to zero but it builds up during the evolution of the system, as shown in Fig. 3 a). The corresponding values of the transverse four-velocity  $u_r$  are plotted in the part b). To check if the flow approaches the asymptotic scaling solution, we compare the velocity profiles calculated numerically at different times  $t_i = 1, 4, 7, 10, 13, 16 \text{ fm}$  (solid lines) with the ideal Hubble-like velocities of the form  $r/t_i$  (thin dashed lines) in the regions  $r < t_i$ . As expected, in the case  $H = 0$  the calculated profiles do not agree with the ideal curves in the considered evolution times.

In the part c) of Fig. 3 we observe that the central part of the system cools down very fast from  $T = 2T_c$  down to the critical temperature  $T = T_c$  and the subsequent cooling is very much slowed down. This behavior is caused by different values of the sound velocity in the regions above and below  $T_c$ ; larger values of  $c_s$  in the plasma phase imply its faster cooling. We note that for the first order phase transition the speed of sound drops to zero at  $T = T_c$  and the system keeps on expanding at a constant temperature of  $T = T_c$ . In the present case we deal with a sudden cross-over transition, hence the expansion of the volume is coupled to a small decrease of the temperature. From Fig. 3 d) showing the isotherms in the  $t - r$  space, we may conclude that expansion of the system without noticeable cooling below  $T_c$  takes more than 20 fm.

The evolution of matter shown in Fig. 3 may be confronted with the situation where the non-zero pre-equilibrium flow is included in the initial condition. In Fig. 4 we show our results obtained in the case  $H = 0.25 \text{ fm}^{-1}$ , with

the same initial central temperature  $T_0 = 2T_c$ . Since the transverse flow is present already at the beginning of the evolution, the expansion of the system is much faster than that discussed in the previous case of  $H = 0$ . In Fig. 4 a) we show the velocity profiles in  $r$ , again for 6 different values of time. By comparing to the ideal curves of the form  $r/t_i$  (thin dashed lines) we observe that the flow approaches the asymptotic scaling solution after about 7 fm.

In Fig. 4 c) we can see similar behavior to that presented in Fig. 3 c), namely, the initial fast cooling of the hot center, which is slowed down when the system approaches  $T_c$ . We observe, however, that in the case  $H = 0.25 \text{ fm}^{-1}$  the slowing down of the cooling process is not as much effective as that observed in the case  $H = 0$ . Due to the larger transverse flow, the energy from the interior is transported outside, the temperature in the center continues to drop down, and a very interesting situation happens: the parts of the system away from the center become hotter than the parts in the center. This phenomenon is well seen in Fig. 4 d) where the isotherms of the system are shown. We note that isotherms of similar shape are used in the Cracow model where they are defined by the condition of constant proper time  $\tau$  [2]. On the other hand, the Blast-Wave model assumes that freeze-out happens at a constant value of the ordinary time  $t$  with a fixed temperature  $T$ ; whereas the Buda-Lund model assumes that the temperature profile may eventually decrease to 0 at large transverse extensions, hence capturing the feature that the temperature vanishes for very large transverse coordinates in all of the presented calculations.

In Fig. 5 we show a collection of the velocity profiles obtained for four different values of the parameter  $H$  and for three different values of the central temperature  $T_0$ . The four rows of smaller figures describe the results obtained with  $H = 0, 0.10, 0.25, 1.0 \text{ fm}^{-1}$ , while the three columns correspond to the central temperature  $T_0 = 1.5T_c$ ,  $T_0 = 2T_c$ , and  $T_0 = 3T_c$ .

The results presented in Fig. 5 are obtained with the analytic model for the temperature dependence of the sound velocity, hence, by comparison of Fig. 5 with the two previous figures, the effects of the change of the function  $c_s(T)$  on the time evolution of the system may be observed. For example, comparing the part c2) of Fig. 5 with the part a) of Fig. 4 (both results obtained with  $H = 0.25 \text{ fm}^{-1}$  and  $T_0 = 2T_c$ ) we can see that the flow obtained with the analytic model is closer to the asymptotic scaling form than the flow obtained for the lattice equation of state. We note that the main difference between the two cases is that the sound velocity in the analytic model is smaller in the hadronic phase. The asymptotic scaling solutions are more easily generated at the reduced values of the sound velocity as shown in Refs. [10, 22, 23]. This effect explains a better agreement of the generated transverse flow with the asymptotic scaling solution obtained in the analytic model.

Let us now discuss the impact of the initial temperature on the formation of the transverse flow. Since the spatial extension of the system is the same in all considered cases (roughly a diameter of the gold nucleus), a higher initial temperature implies a larger pressure gradient leading directly to the formation of the stronger flow. This effect is seen in Fig. 5 if the results obtained with the same value of  $H$  but different values of  $T_0$  are compared. The presence of the pre-equilibrium transverse flow also helps to develop the strong transverse flow, and this effect is added to the effects of the pressure gradient. This is clearly seen in the case  $H = 0.10 \text{ fm}^{-1}$ , depicted in the parts b1) - b3) of Fig. 5. At  $t = 16$  fm the flow in the range  $r < 10$  fm is close but below the asymptotic scaling solution for  $T_0 = 2T_c$ , and close but above the asymptotic scaling solution for  $T_0 = 3T_c$ . For  $T_0 = 1.5T_c$  the flow is noticeably below the asymptotic scaling form. We conclude that the asymptotic solution may be reached either from above or from below (in the region  $r \ll t$ ), depending on the value of the initial temperature. If the pre-equilibrium flow is strong enough the asymptotic solution is approached from above. This behavior is indicated by our results obtained in the cases  $H = 0.25 \text{ fm}^{-1}$  and  $H = 1.0 \text{ fm}^{-1}$ , Fig. 5 c1) - d3). Interestingly, in the case  $H = 1/t_0 = 1.0 \text{ fm}^{-1}$ , where the initial flow agrees with the scaling form already at the beginning of the time evolution, the pressure gradient accelerates the matter and the convergence to the scaling form is delayed. On the other hand, the existence of a non-zero pre-equilibrium flow seems to be a necessary condition for the formation of the accelerationless Hubble-like flows in the evolution times of 10-15 fm. This is indicated by our results obtained with  $H = 0$  for different values of  $T_0$ , Fig. 5 a1) - a3). The amount of the pre-equilibrium flow required to achieve the fast convergence to the asymptotic solution depends on the initial temperature (pressure gradient); smaller values of  $H$  may be compensated by larger values of  $T_0$ . For example, at  $t = 16$  fm the flow profiles are very similar in the cases:  $H = 1 \text{ fm}^{-1}$  and  $T = 1.5T_0$  (part d1),  $H = 0.25 \text{ fm}^{-1}$  and  $T = 2T_c$  (part c2), and also  $H = 0.1 \text{ fm}^{-1}$  and  $T = 3T_c$  (part b3). It is quite remarkable, that the presence of this pre-equilibrium flow is required only to set the value of the Hubble constant to  $H = 1/t$  i.e. to reach the *asymptotic* scaling solution within a short time period, however, we find that the linear flow profile,  $v = Hr$  develops with  $H \neq 1/t$  in all the considered cases by about 7 fm/c, regardless of the details of the initial conditions.

## VI. CONCLUSIONS

Our results show a dynamical development of the scaling solutions in the relativistic hydrodynamics applied to relativistic heavy-ion collisions. For the realistic initial conditions connecting the amount of the initially produced entropy with the number of participating nucleons, we find that a Hubble type linear transverse flow, characterized

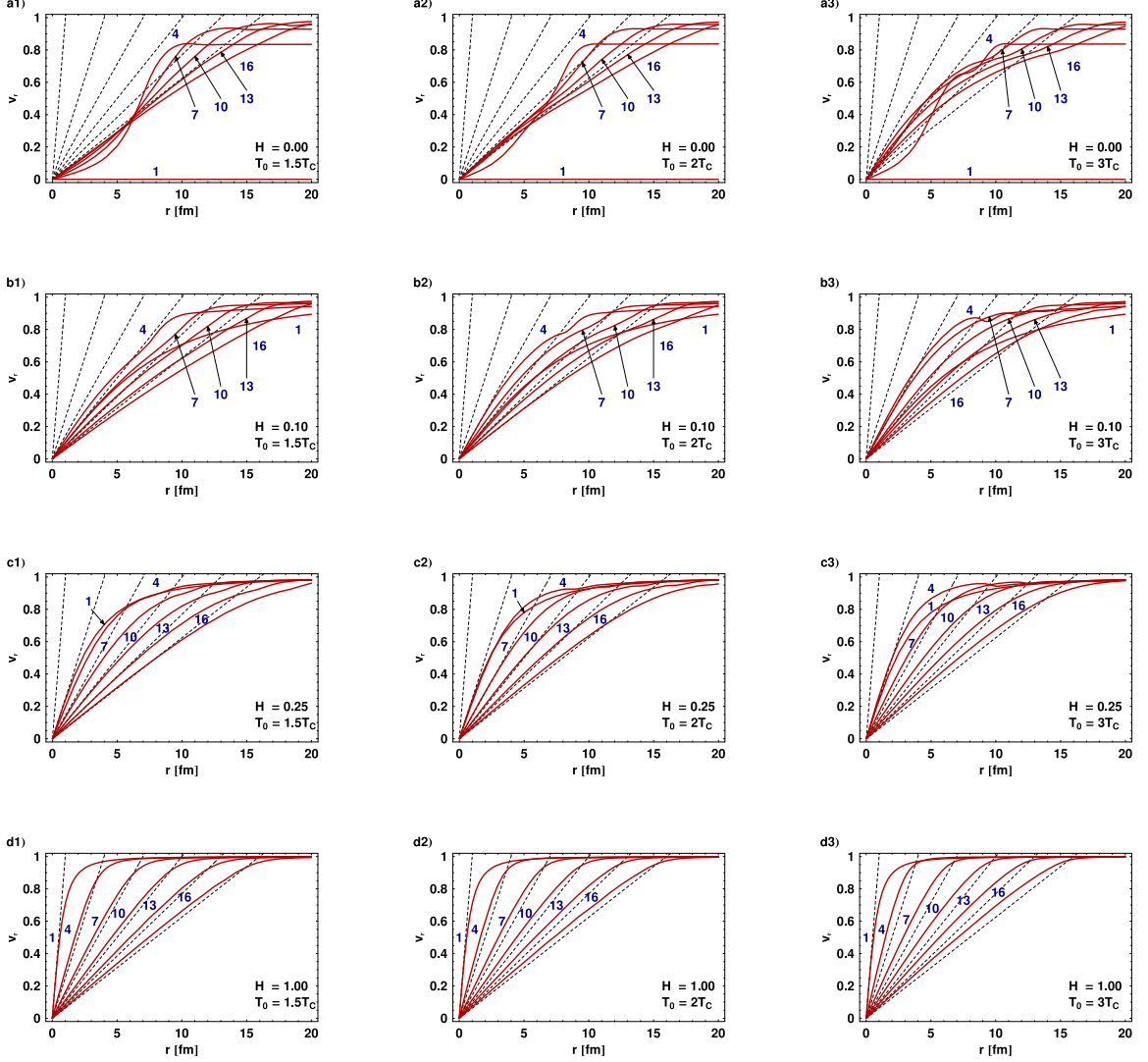


FIG. 5: Velocity profiles in  $r$  (solid lines) calculated for different values of the parameter  $H$  and different values of the initial central temperature  $T_0$ . The labels 1,4,7,10,13 and 16 denote the evolution time in fm. The values of  $H$  are given in 1/fm. The thin dashed lines show the ideal profiles of the form  $r/t$  obtained for the same values of time.

by  $v = Hr$  develops by about 7 fm/c regardless of the details of the initial conditions when varied numerically in a reasonable range. However, it is more difficult for the transverse flow to achieve the *asymptotic*, accelerationless scaling form: to reach the values of  $H = 1/t$  within the evolution time of about 10 -15 fm. For this, the necessary conditions are thus stronger: pre-equilibrium transverse flow has to be present already at the beginning of the hydrodynamic evolution at the initial time of 1 fm. The amount of the pre-equilibrium flow, required for the fast approach to the asymptotic solutions, depends on the initial pressure gradients; for larger gradients smaller initial flows are necessary.

The results of these calculations give support for using the phenomenological parameterizations of the freeze-out process such as the Blast-Wave, Buda-Lund, and Cracow models. Certainly, more work should be done to combine the output of the hydrodynamic calculations with the description of freeze-out used in these models, however, we showed that such features as the linear flow profiles or the isotherms defined by the constant value of the proper time appear as the solutions of the relativistic hydrodynamics with suitably chosen initial conditions.

### Acknowledgments

This work was supported in part by the Polish State Committee of Scientific Research, grant 2 P03B 05925, by the Hungarian OTKA grant T038406, the MTA - OTKA - NSF grant INT0089462 and by the exchange program of the Hungarian and Polish Academy of Sciences as well as by the Polish KBN - Hungarian Ministry of Education Exchange Programme in Science and Technology.

---

[1] QM02, Nucl. Phys., **A715**, Proc. of the 16th Int. Conf. on Ultra-Relativistic Nucleus-Nucleus Collisions, Nantes, France.

[2] W. Broniowski, W. Florkowski, Phys. Rev. Lett., **87** (2001) 272302, nucl-th/0106050.

[3] W. Broniowski, W. Florkowski, Phys. Rev., **C65** (2002) 064905, nucl-th/0112043.

[4] M. Csanad, T. Cs org , B. L rstad, A. Ster, J. Phys., **G30** (2004) S1079–S1082, nucl-th/0403074.

[5] J. Allday, “Quarks, Leptons and the Big Bang”, IOP Publishing Ltd 2002, ISBN 0 7503 0806 0

[6] J. P. Bondorf, S. I. A. Garpman and J. Zim nyi, Nucl. Phys. **A296** (1978) 320–332

[7] L. D. Landau, Izv. Akad. Nauk SSSR Ser. Fiz., **17** (1953) 51–64.

[8] S. Z. Belenkij, L. D. Landau, Nuovo Cim. Suppl., **3S10** (1956) 15.

[9] F. Cooper, G. Frye, E. Schonberg, Phys. Rev. Lett., **32** (1974) 862.

[10] F. Cooper, G. Frye, E. Schonberg, Phys. Rev., **D11** (1975) 192.

[11] J. D. Bjorken, Phys. Rev., **D27** (1983) 140–151.

[12] G. Baym, B. L. Friman, J. P. Blaizot, M. Soyeur, W. Czyz, Nucl. Phys., **A407** (1983) 541–570.

[13] R. C. Hwa, Phys. Rev., **D10** (1974) 2260.

[14] C. B. Chiu, K.-H. Wang, Phys. Rev., **D12** (1975) 272.

[15] C. B. Chiu, E. C. G. Sudarshan, K.-H. Wang, Phys. Rev., **D12** (1975) 902.

[16] M. I. Gorenstein, Y. M. Sinyukov, V. I. Zhdanov, Phys. Lett., **B71** (1977) 199–202.

[17] M. I. Gorenstein, Y. M. Sinyukov, V. I. Zhdanov, Zh. Eksp. Teor. Fiz., **74** (1978) 833–845.

[18] P. Huovinen, Acta Phys. Polon., **B33** (2002) 1635–1650, nucl-th/0204029.

[19] P. F. Kolb, U. Heinz, nucl-th/0305084.

[20] D. Teaney, J. Lauret, E. V. Shuryak, nucl-th/0110037.

[21] T. Hirano, J. Phys., **G30** (2004) S845–S852, nucl-th/0403042.

[22] T. S. Biro, Phys. Lett., **B474** (2000) 21–26, nucl-th/9911004.

[23] T. S. Biro, Phys. Lett., **B487** (2000) 133–139, nucl-th/0003027.

[24] T. Cs org , F. Grassi, Y. Hama, T. Kodama, Heavy Ion Physics, **A21** (2004) 53–62, hep-ph/0203204.

[25] T. Cs org , F. Grassi, Y. Hama, T. Kodama, Heavy Ion Physics, **A21** (2004) 63–71, hep-ph/0204300.

[26] T. Cs org , F. Grassi, Y. Hama, T. Kodama, Phys. Lett., **B565** (2003) 107–115, nucl-th/0305059.

[27] T. Cs org , L. P. Csernai, Y. Hama, T. Kodama, Heavy Ion Physics, **A21** (2004) 73–84, nucl-th/0306004.

[28] F. Retiere, M. A. Lisa, nucl-th/0312024.

[29] F. Retiere, J. Phys., **G30** (2004) S827–S834, nucl-ex/0405024.

[30] A. N. Makhlin, Y. M. Sinyukov, Z. Phys., **C39** (1988) 69.

[31] P. F. Kolb, R. Rapp, Phys. Rev., **C67** (2003) 044903, hep-ph/0210222.

[32] S. V. Akkelin, T. Cs org , B. Luk cs, Y. M. Sinyukov, M. Weiner, Phys. Lett., **B505** (2001) 64–70, hep-ph/0012127.

[33] T. Cs org , Central European Journal of Physics, **2** (4) (2004) 1–10, hep-ph/0111139.

[34] T. Cs org , S. V. Akkelin, Y. Hama, B. Luk cs, Y. M. Sinyukov, Phys. Rev., **C67** (2003) 034904, hep-ph/0108067.

[35] I. G. Bearden, *et al.*, BRAHMS, Phys. Rev. Lett., **90** (2003) 102301.

[36] I. G. Bearden, BRAHMS, nucl-ex/0403050.

[37] W. Florkowski, W. Broniowski, M. Michalec, Acta Phys. Polon., **B33** (2002) 761–769, nucl-th/0106009.

[38] G. Torrieri, W. Broniowski, W. Florkowski, J. Letessier, J. Rafelski, nucl-th/0404083.

[39] B. Mohanty, J.-e. Alam, Phys. Rev., **C68** (2003) 064903, nucl-th/0301086.

[40] F. Karsch, Nucl. Phys., **A698** (2002) 199–208, hep-ph/0103314.

[41] K. K. Szab , A. I. T th, JHEP, **06** (2003) 008, hep-ph/0302255.

[42] W. Broniowski, W. Florkowski, Phys. Lett., **B490** (2000) 223–227, hep-ph/0004104.

[43] W. Broniowski, hep-ph/0008112.

[44] W. Broniowski, W. Florkowski, L. Y. Glozman, hep-ph/0407290.

[45] R. Hagedorn, Nuovo Cim. Suppl., **3** (1965) 147–186.

[46] D. Prorok, Acta Phys. Polon., **B33** (2002) 1583–1600, hep-ph/0205221.